

Supplementary information

A gel electrolyte-based direct seawater electrolysis

Wenbin Tang^{1,2,4}, Zhiyu Zhao^{*1,2,3,4}, Dongsheng Yang^{1,3,4}, YanHao Liu^b, Liangyu Zhu^{2,3,4}, Yue Wu⁵, Cheng Lan^{1,2,3,4}, Wenchuan Jiang^{1,2,3,4}, Yifan Wu^{1,2,3,4}, Tao Liu^{*1,2,3,4}, Heping Xie^{*1,2,3,4,6}

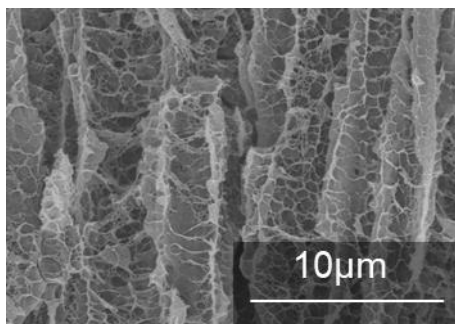
1. State Key Laboratory of Intelligent Construction and Healthy Operation and Maintenance of Deep Underground Engineering, College of Polymer Science and Engineering, Sichuan University & Shenzhen University, Chengdu 610065, China.
2. Institute of New Energy and Low-Carbon Technology, Sichuan University, Chengdu 610065, China.
3. Guangdong Provincial Key Laboratory of Deep Earth Sciences and Geothermal Energy Exploitation and Utilization, College of Civil and Transportation Engineering, Shenzhen University, Shenzhen 518060, China.
4. Shenzhen Key Laboratory of Deep Engineering Science and Green Energy, Institute of Deep Earth Sciences and Green Energy, Shenzhen University, Shenzhen 518060, China.
5. School of Chemical Engineering, Sichuan University, Chengdu 610065, China.
6. Lead Contact.

Correspondence should be addressed to Heping Xie: xiehp@scu.edu.cn.

Tao Liu: liutao3200023@scu.edu.cn.

Zhiyu Zhao: 471960678@qq.com

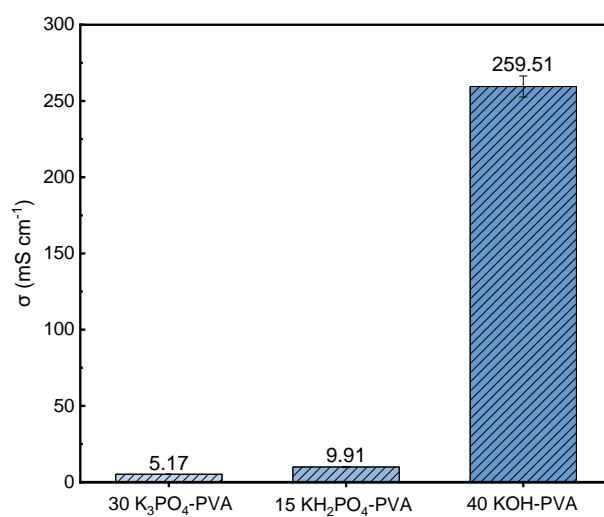
Supplementary Figures



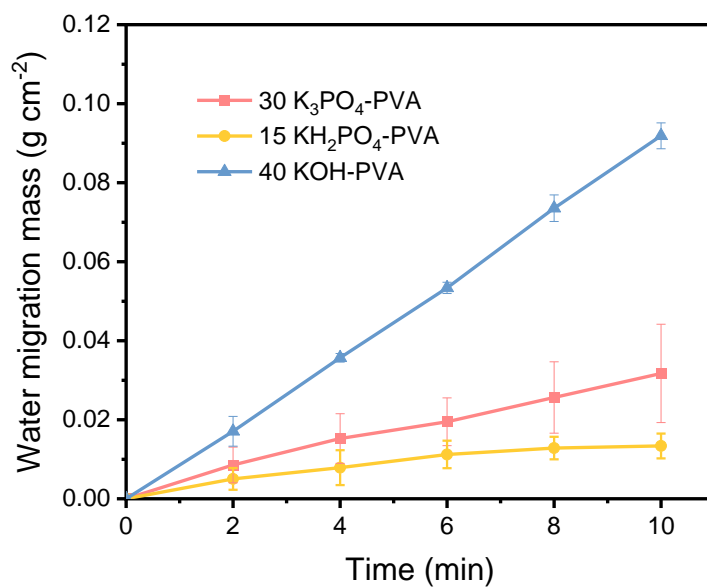
Supplementary Figure 1. Cross-section SEM of 40 KOH-PVA.



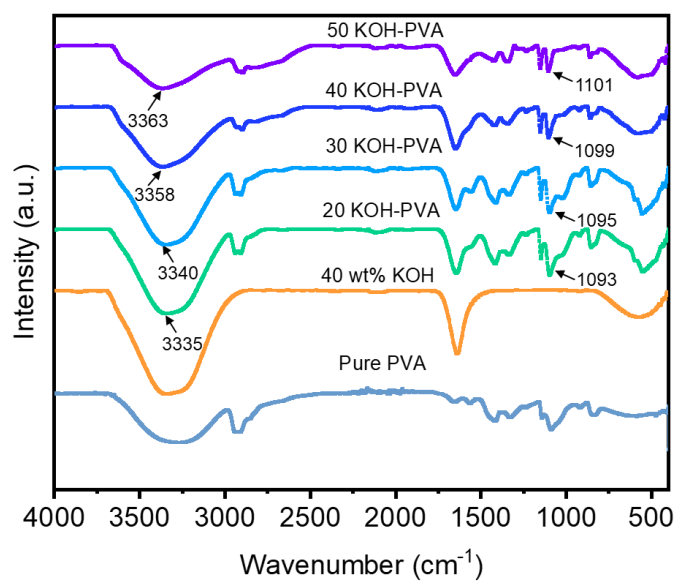
Supplementary Figure 2. Gel electrolytes of different shapes.



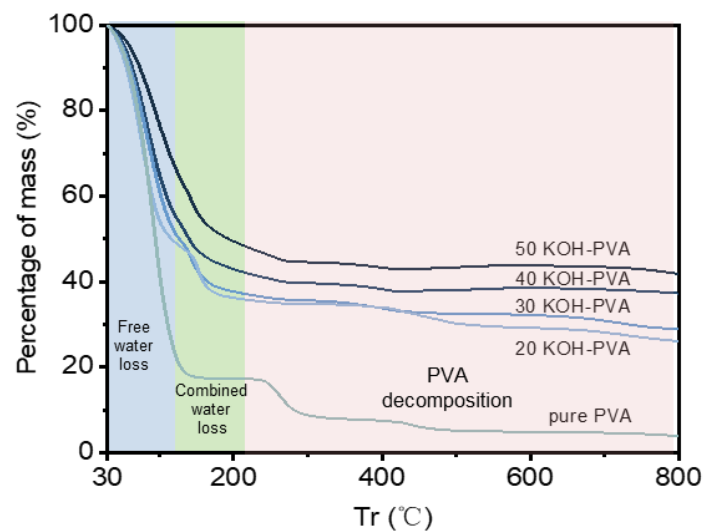
Supplementary Figure 3. Ionic conductivity of different gel electrolytes.



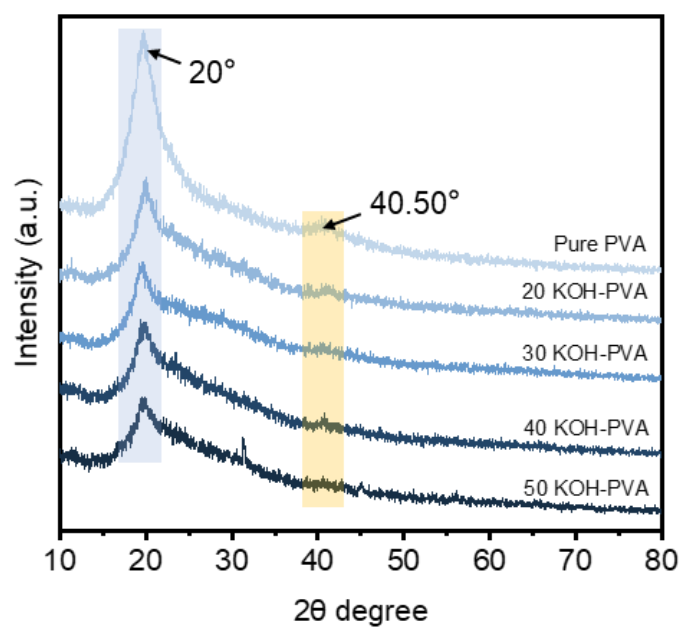
Supplementary Figure 4. Water migration curve of different gel electrolytes.



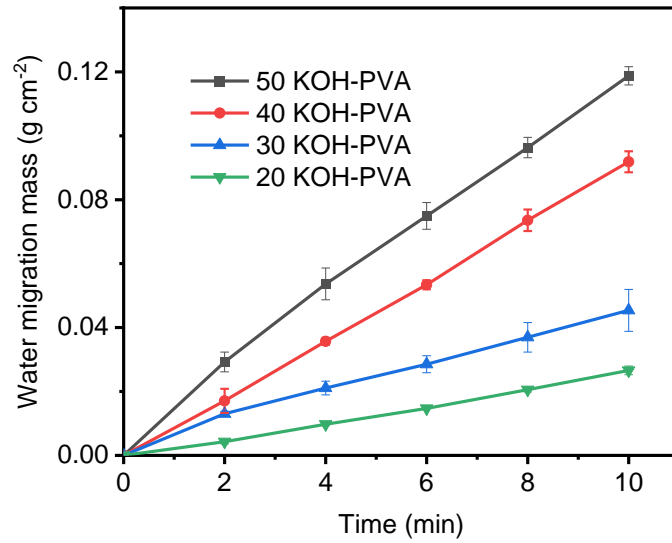
Supplementary Figure 5. ATR-FTIR spectra of pure PVA, 40 wt% KOH solution and gel electrolytes prepared by different KOH concentration.



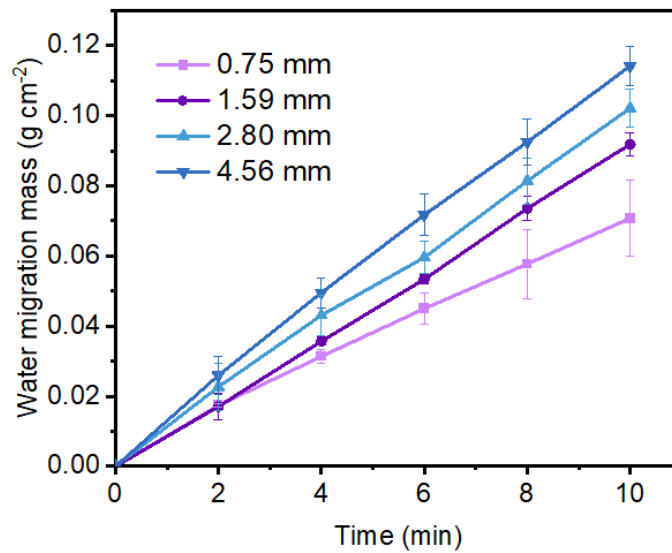
Supplementary Figure 6. Thermogravimetric analysis (TGA) curves of pure PVA and gel electrolytes prepared by different KOH concentration.



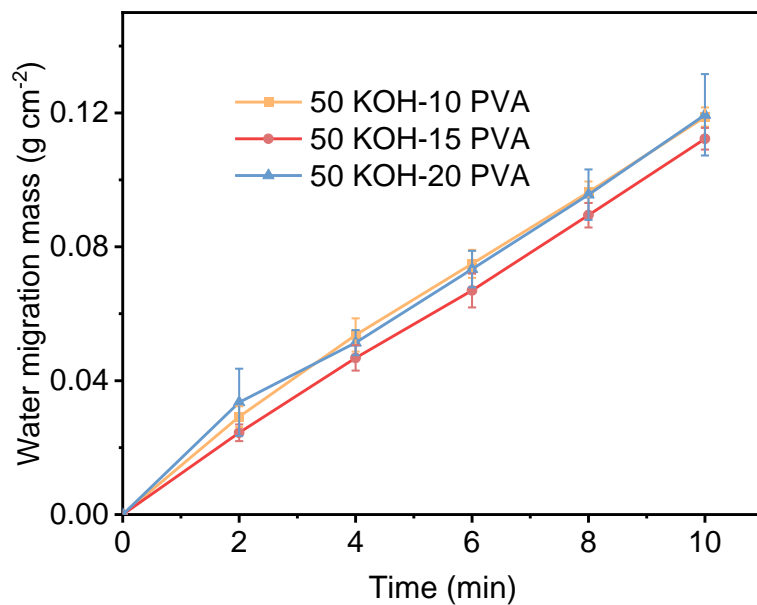
Supplementary Figure 7. X-ray diffraction patterns of gel electrolytes prepared by different KOH concentration.



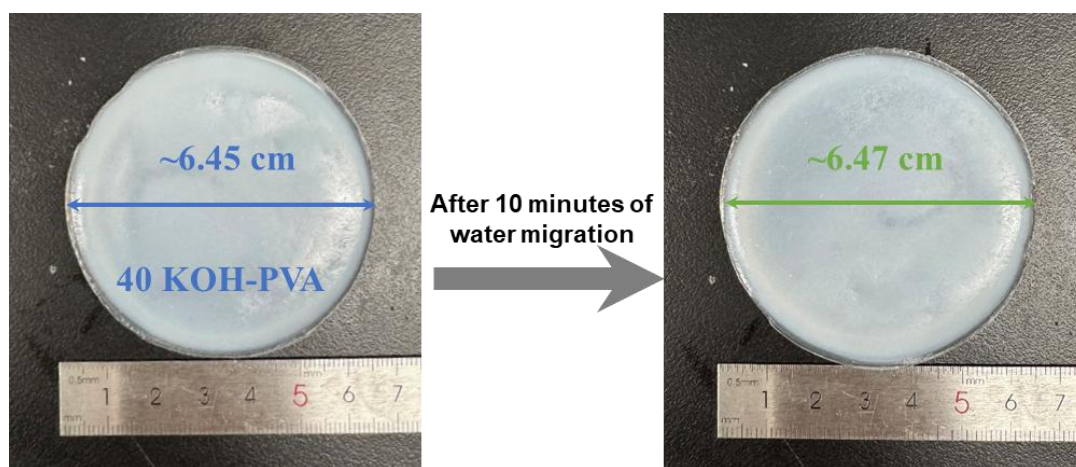
Supplementary Figure 8. Water migration curves. The 0.5 M NaCl solution was simulated seawater; 20 KOH-PVA, 30 KOH-PVA, 40 KOH-PVA, 50 KOH-PVA were selected as gel electrolytes.



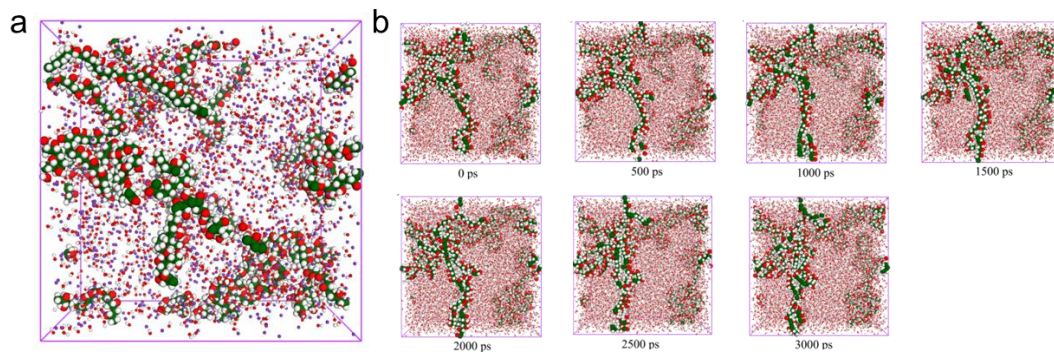
Supplementary Figure 9. Water migration curves. The 0.5 M NaCl solution was simulated seawater; 40 KOH-PVA with different thickness were selected as gel electrolytes.



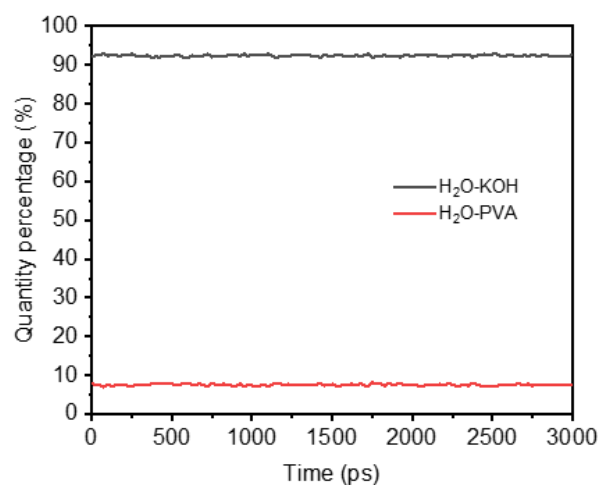
Supplementary Figure 10. Water migration curves. The 0.5 M NaCl solution was simulated seawater; 50 KOH-10 PVA, 50 KOH-15 PVA, 50 KOH-20 PVA were selected as gel electrolytes.



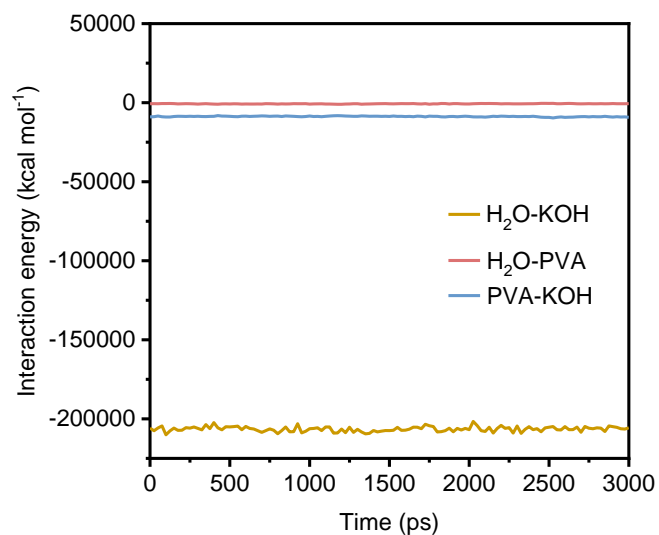
Supplementary Figure 11. The dimensional changes of 40 KOH-PVA after water migration.



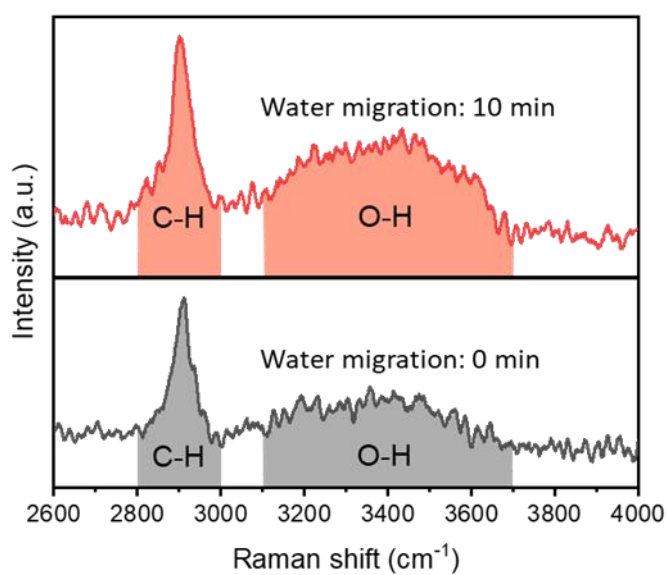
Supplementary Figure 12. **a**, Initial models of PVA-KOH gel. C atoms shown in deep green, K in purple, O in red, and H in white. For clarity, H₂O molecules are not shown. **b**, Evolution of system configuration over 3000 ps simulation period. C atoms are shown in deep green, O in red, and H in white. For clarity, KOH molecules are not shown.



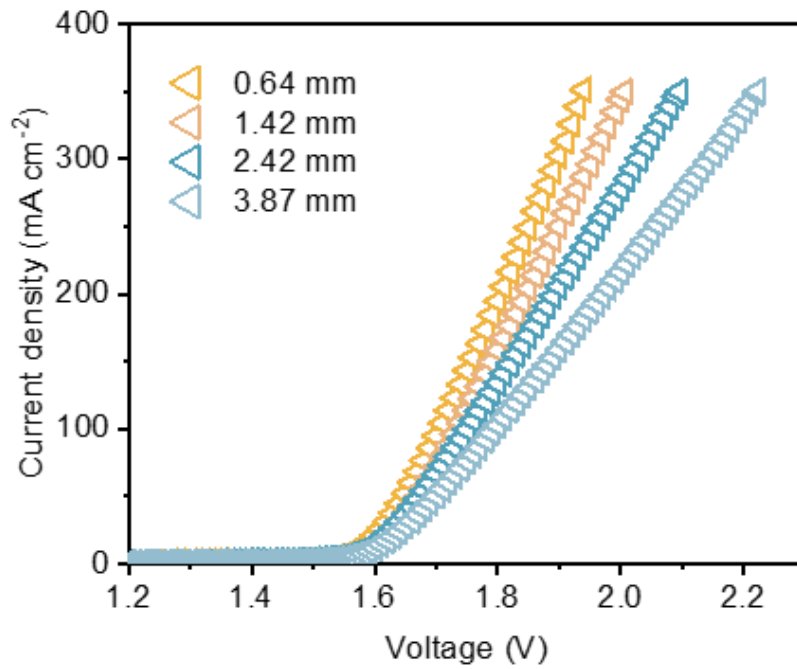
Supplementary Figure 13. The percentage of hydrogen bonds formed between H₂O and KOH and PVA, respectively, during the observed time.



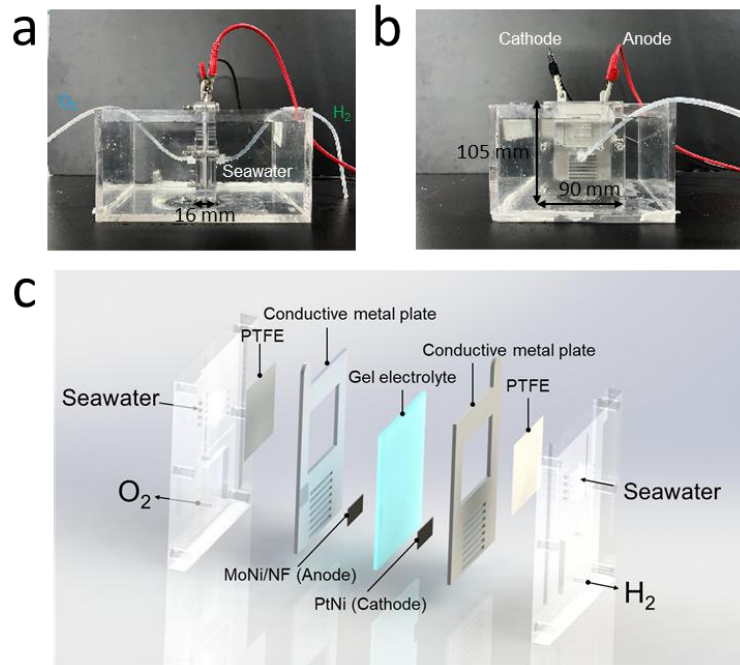
Supplementary Figure 14. Binding energy of hydrogen bonds formed between water molecules, PVA and KOH.



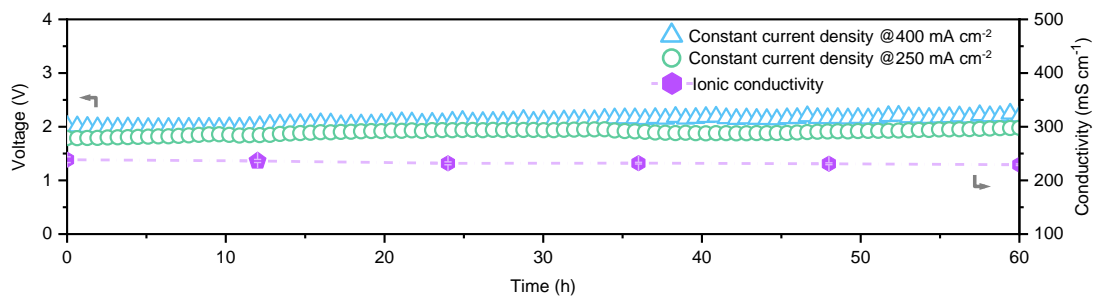
Supplementary Figure 15. Raman spectra of KOH-PVA gel electrolyte surface.



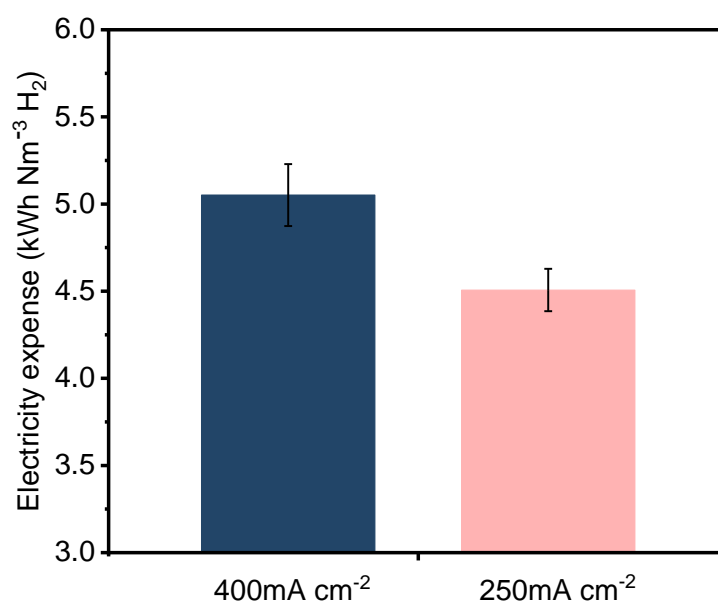
Supplementary Figure 16. LSV curves of 40 KOH-PVA electrolyte membranes with different thickness.



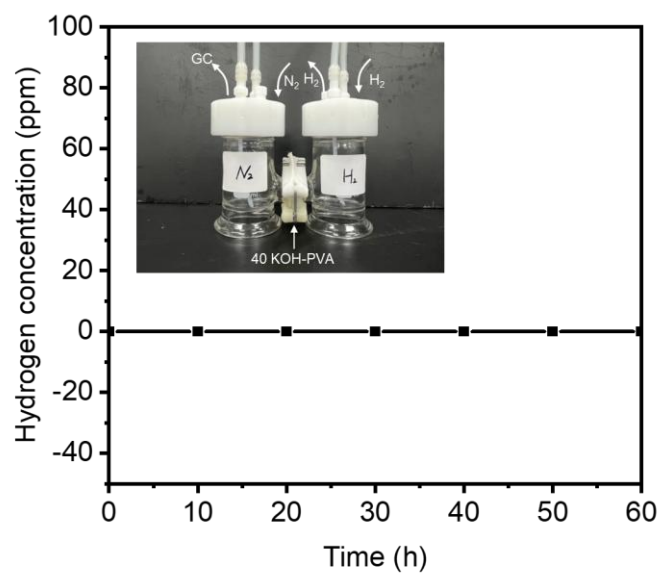
Supplementary Figure 17. Diagram of (a) side, (b) front and (c) three-dimensional components of the KOH-PVA gel seawater direct electrolysis hydrogen production unit.



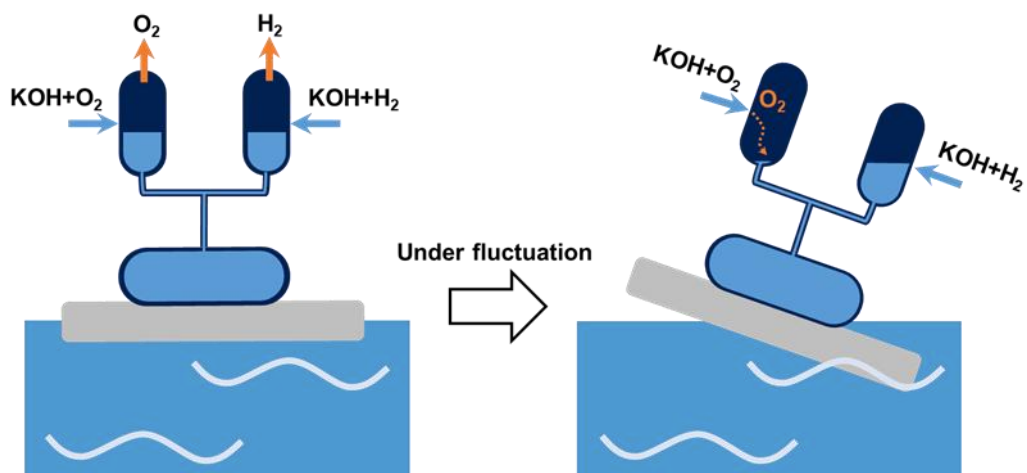
Supplementary Figure 18. Hydrogen production voltage and ion conductivity stability test for direct seawater electrolysis using 40 KOH-PVA.



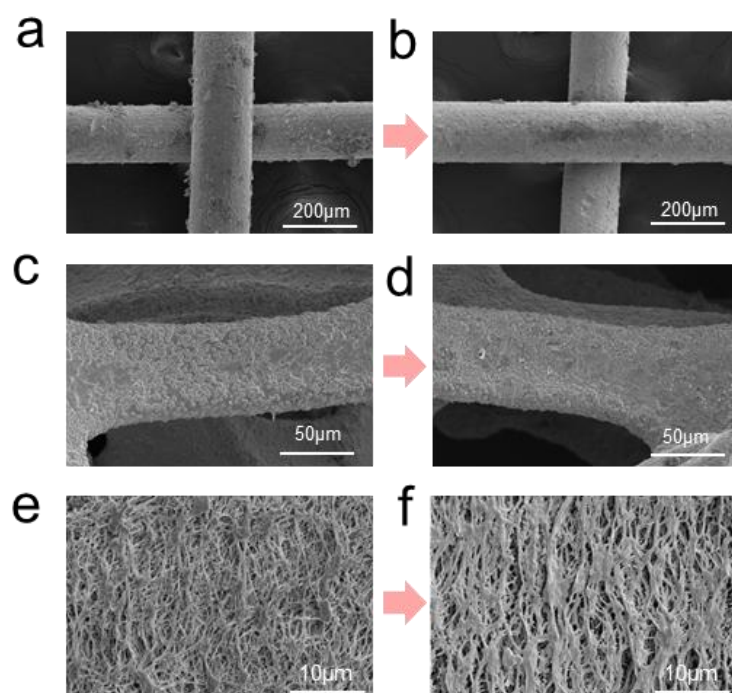
Supplementary Figure 19. Energy consumption for hydrogen production by direct seawater electrolysis with 40 KOH-PVA gel electrolyte at 250 and 400 mA·cm⁻² current densities.



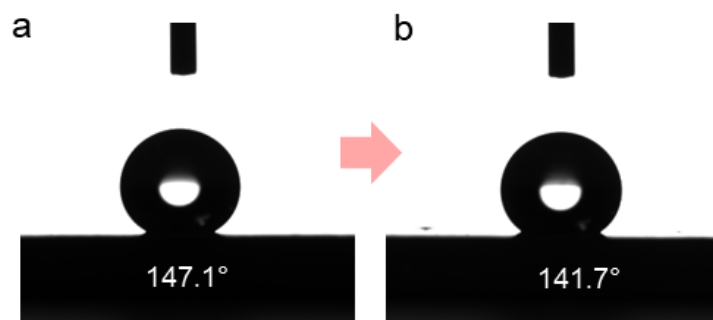
Supplementary Figure 20. The hydrogen permeation concentration of 40 KOH-PVA membrane was measured by gas chromatography for 60 hours.



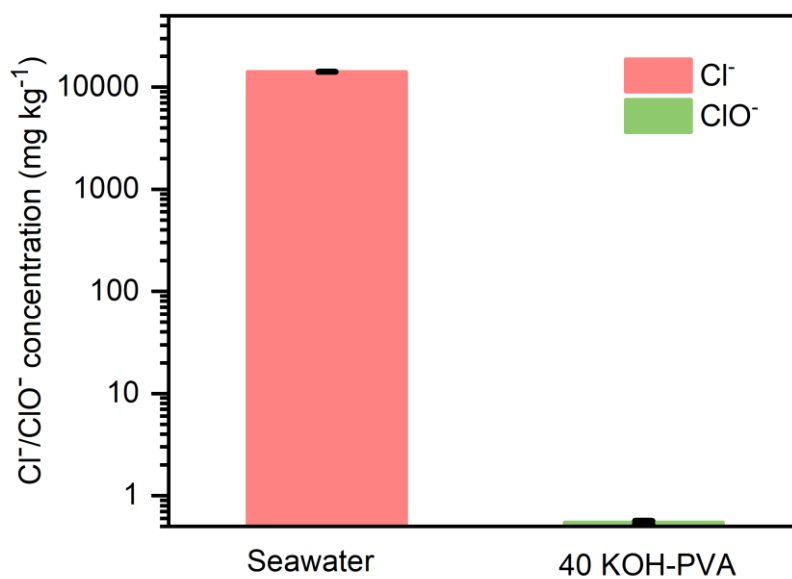
Supplementary Figure 21. Under fluctuating conditions, hydrogen and oxygen crossover may occur due to liquid surface tilt in conventional electrolysis systems based on liquid electrolytes.



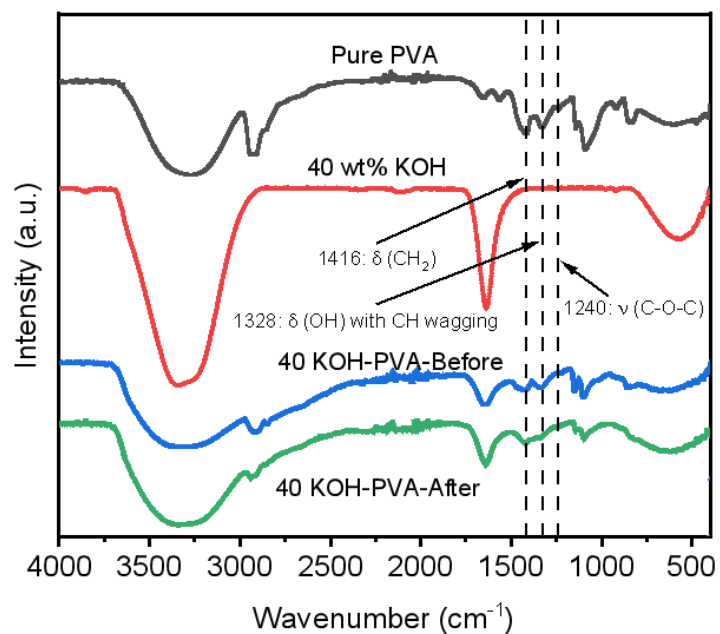
Supplementary Figure 22. Electron microscopic photos of cathode catalyst (a, b), anode catalyst (c, d) and PTFE film (e, f) before and after hydrogen production by direct electrolysis of seawater with gel electrolyte.



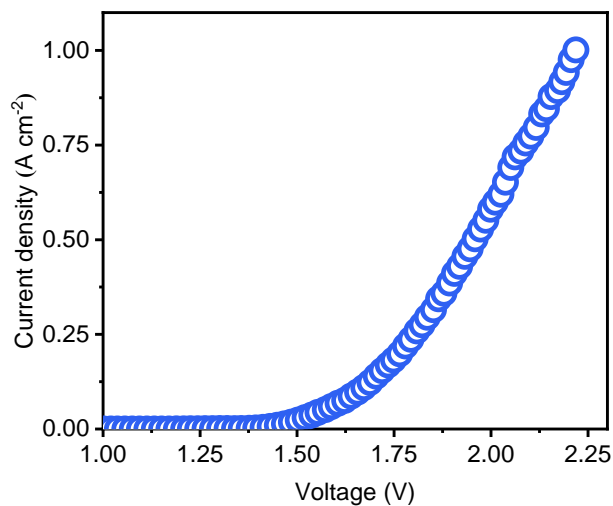
Supplementary Figure 23. Contact Angle between PTFE film and seawater before (a) and after (b) 60 hours of hydrogen production by electrolysis.



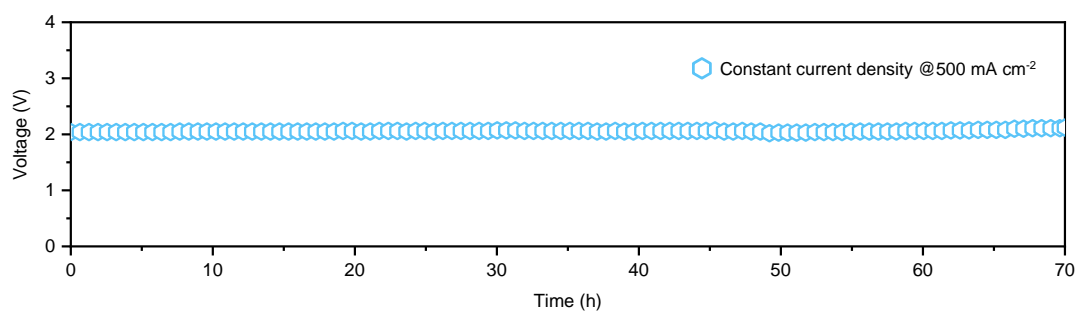
Supplementary Figure 24. Cl^- content in seawater and hypochlorite ClO^- content in gel after long-term electrolysis.



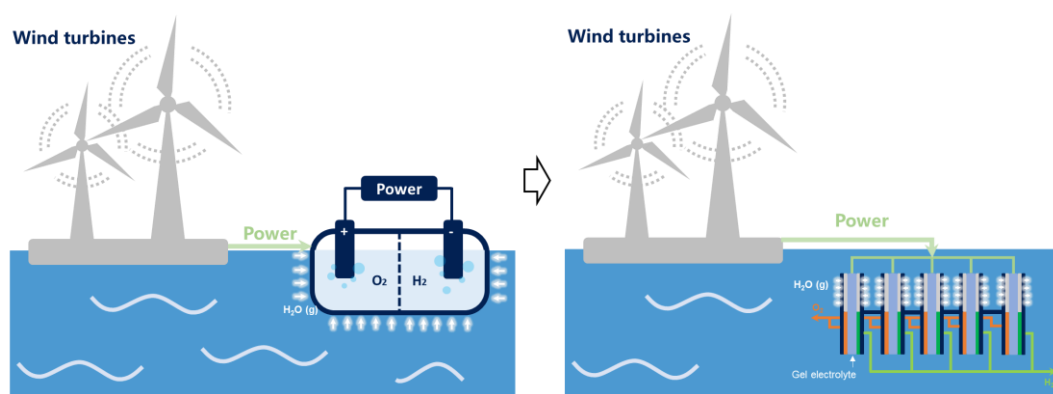
Supplementary Figure 25. Infrared spectrum of pure PVA, KOH solution and gel electrolyte before and after electrolysis.



Supplementary Figure 26. LSV curve of 40 KOH-PVA.



Supplementary Figure 27. Durability test for seawater electrolysis at 500 mA cm⁻².



Supplementary Figure 28. Large-scale hydrogen production from seawater is achieved through the superposition of multiple groups of single devices.